

The Asian Dust Detection Algorithm using NOAA/AVHRR Data

Dodi Sudiana, Hiroaki Kuze, Nobuo Takeuchi

Center for Environmental Remote Sensing (CEReS), Chiba University

1-33 Yayoi-cho, Inage-ku, Chiba 263-8522

Tel./Fax. +81-43-290-3852

E-mail: dodi@ceres.cr.chiba-u.ac.jp

Abstract. On April 15, 1998 an intense dust storm began in the western Chinese province of Xinjiang and Mongolia. These annual phenomena have been closely monitored by many scientists using satellite, aircraft and surface-based measurements. The Asian dust, or kosa, was transported to the east coast of China and within several days may move across the Pacific impacting the west coast of America. The analysis presented in this paper describes the algorithm of Asian dust detection utilizing parameter related to the brightness temperature of channel 4 and 5 of NOAA/AVHRR data. The results, in terms of the AVI (Aerosol Vapor Index), showed a good relationship with aerosol optical thickness derived from TOMS data and the surface-based measurements.

1. Introduction

Dust storms in deserts in East Asia tend to cause major aerosol events well beyond the Asia continent. Dust clouds are formed when the friction from high surface wind speeds ($> 5\text{m/s}$) lifts loose dust particles into the atmospheric boundary layer or above [1]. Wind blown dust originating from the arid deserts of Mongolia and China is a well-known springtime meteorological phenomenon throughout East Asia. In fact, Asian dust meteorological conditions are sufficiently common to have acquired local names: huangha in China, whangsa in Korea, and kosa in Japan.

The transport of desert dust from Asia to the North Pacific atmosphere is well documented [e.g. 2,3,4,5] and results in a maximum in aerosol loading each spring. Over the Pacific, the concentration of species from anthropogenic sources in Asia was also found to be enhanced during spring [6,7,8] and have been documented to reach North America [7].

The Asian dust storms have been studied for decades to understand their sources, mechanism of transport, and aerosol characteristics, including the effects on radiation. [2,3,4,5]. However, quantitative understanding of individual dust events, e.g. the dust emission locations and rates as well as the details of long-range transport and removal, are still incomplete.

In this paper, we presented a method to recognize the Asian dust events using NOAA/AVHRR thermal channels in the 1998 events. The brightness temperature difference of AVHRR channel 4 and 5 of the NOAA was

proved to be effective in detecting the extension of the Asian dust aerosol. Observed were the dense dust above the Chinese continent, and its transportation towards the east, extending and diffusing with time, over the Yellow sea, Korea and Japanese Islands to the Pacific Ocean. The source of NOAA/AVHRR was obtained at the receiving station in our center (CEReS, Chiba University).

2. Asian Dust Transport

The April 15, 1998 dust cloud followed a southern route toward central and eastern China and subsequently turned toward Korea to the north. The location of the dust plume is visualized using the daily dust patterns, which derived from the SeaWiFS images, GOES 9 and GOES 10 images and TOMS absorbing aerosol index data. Over the Pacific Ocean, the dust cloud followed the path of the springtime East-Asian aerosol plume shown by the contours of the optical thickness derived from AVHRR data as shown in Figure 1.

3. Asian Dust Detection method

The split window method to take the difference of brightness temperature of AVHRR-channel 4 and 5 has been utilized to estimate vapor amount to get the sea surface temperature. Since the opposite emissivity difference of lithic dust/aerosol in 11 and 12 micron bands against vapor, it is useful to detect Asian dust (kosa). This method has been applied to detect volcanic clouds and discriminate them from water/ice clouds.

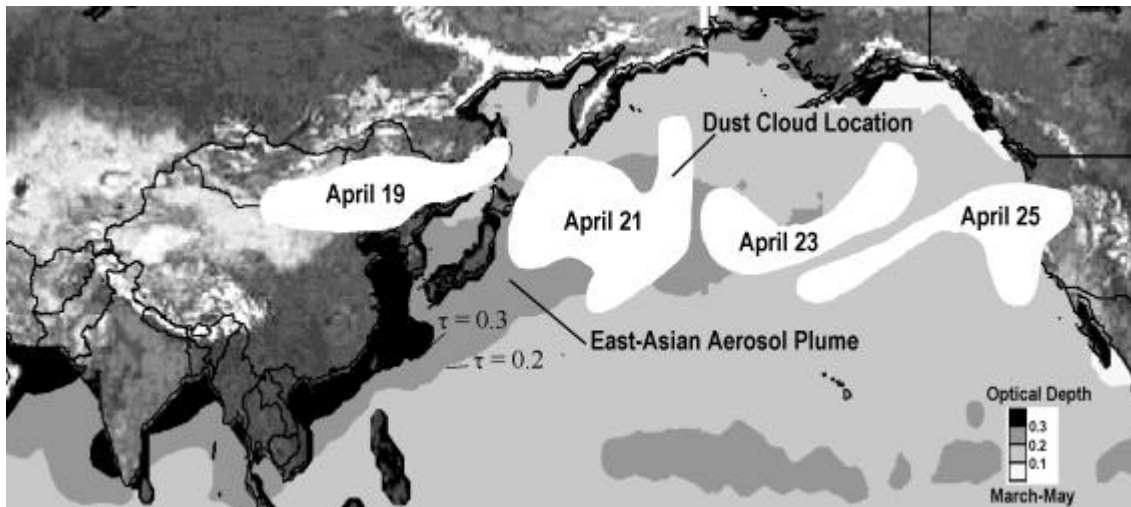


Figure 1. Approximate location of the April dust cloud over the Pacific Ocean between 21-25 April.

Step 1. The raw data of AVHRR (11b format) are converted into calibrated one, where 10 bit value of $n(i)$ of thermal infrared band i , is computed as radiance using a linear function as follows:

$$E_i = S_i C + I_i \quad (1)$$

where E_i is the radiance value in $\text{mW}/(\text{m}^2\text{-sr}\text{-cm}^{-1})$, and S_i and I_i are respectively the scaled slope and intercept values[9].

Step 2. The calibrated full-scene data are geometrically corrected using GCPs (Geometric Correction Points) originated from the raw (11b format) data.

Step 3. The brightness temperature of channels 4 and 5 is computed using the following formula:

$$T_i(E_i) = \frac{C_2}{\ln\left(1 + \frac{C_1 v^3}{E_i}\right)} \quad (2)$$

where T is the temperature (K) for the radiance value E , v is the central wave number of the channel (cm^{-1}), and C_1 and C_2 are constants ($C_1=1.1910659 \times 10^{-5} \text{ mW}/(\text{m}^2\text{-sr}\text{-cm}^{-4})$ and $C_2=1.438833 \text{ cm}\cdot\text{K}$) [9].

Step 4. The brightness temperature difference of channel 4 and 5 is computed to obtain the Aerosol Vapor Index (AVI) defined as:

$$\text{AVI} = n(5) - n(4) + 200 \quad (3)$$

Where $n(i)$ corresponds to the brightness temperature $t(i)$ in centigrade as:

$$n(i) = 10 + (t(i) - 50) \quad (4)$$

Step 5. The 10 bit data of AVI and AVHRR channels 1-4 in the daytime, or 3-4 in the nighttime, are converted into 16 bits without changing values.

Step 6. The JPEG or GIF images of AVI are obtained with a common scale of the scenes.

In the gray scale images, bright parts corresponds to high AVI domains, i.e. $t(4) \ll t(5)$, where the kosa aerosol is expected to be dense. Figure 2 showed the result of the method.

4. Comparison with TOMS profile data

The data from TOMS record have been used increasingly to understand the behavior of the material within the atmosphere. The TOMS is the first instrument to allow observation of aerosols as the particles cross the land/sea boundary. Using these data it is possible to observe a wide range of phenomena such as desert dust storms, forest fires and biomass burning. To examine the validity of the kosa detection method, we compare the result with the TOMS absorbing aerosol index as shown in Figure 3. In the figure, the high aerosol index value appears in the eastern part of the China

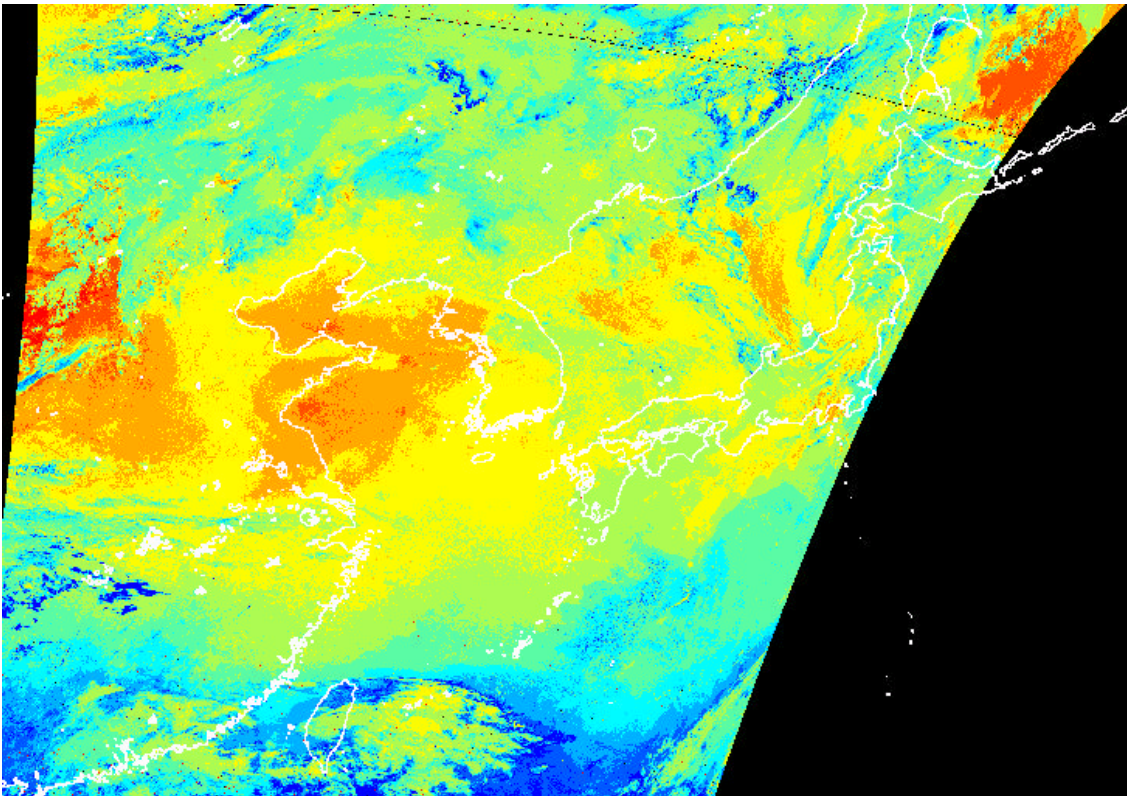
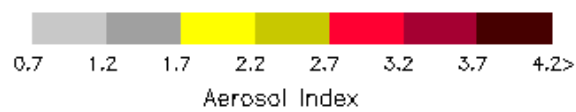
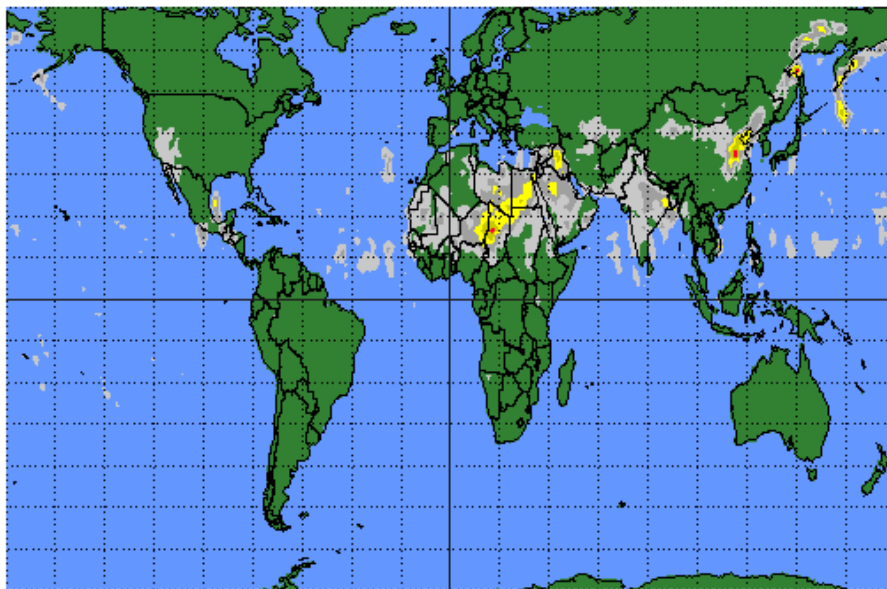


Figure 2. The kosa profile overlaid with coast data



Goddard Space Flight Center

Figure 3. Earth Probe TOMS Aerosol Index global profile.

continent as showed also in reddish part in Figure 2.

The absorbing aerosol index from Earth Probe TOMS is the difference between the measured spectral contrast of the 331 and 360 nm wavelength radiances and the contrast calculated from radiative transfer. The absorbing aerosol index has been shown to have linear relationship to the aerosol optical depth for smoke and dust [10]. The larger aerosol index, the higher the optical depth. TOMS can detect the absorbing aerosols over ocean, all types of land surfaces (including snow or ice [11]), and clouds.

5. Conclusion

The kosa detection method utilizing the brightness temperature difference between channels 4 and 5 of the AVHRR has showed the strong relationship to the TOMS absorbing aerosol index profile.

Reference:

- [1] Gillette, D., A wind tunnel simulation of the erosion of soil: Effect of soil texture, sand-blasting, wind speed, and soil consolidation on the dust production, *Atmos. Environ.*, 12, 1,735-1,743, 1978.
- [2] Mizohata, A. and T. Mamuro, Some information about loess aerosol over Japan, *Japan. Soc. Air Pollut.*, 13, 289-297, 1978.
- [3] Zhou, M., Q. Shaohou, S. Ximing and L. Yuying, Properties of the aerosols during a dust storm over Beijing area, *Acta Scientie Circumstantae*, 1, 207-219, 1981.
- [4] Wang, M. X., J. W. Winchester, T. A. Cahill and L. X. Ren, Chemical elemental composition of windblown dust, 19 April 1980, Beijing, *Kexue Tongbao*, 27, 1193-1198, 1982.
- [5] Iwasaka, Y., H. Minoura and K. Nagaya, The transport and spatial scale of Asian dust-storm clouds: A case study of the dust-storm event of April 1979, *Tellus*, 35B, 189-196, 1983.
- [6] Prospero, J. M. and D. L. Savoie, Effect of continental sources of nitrate concentrations over the Pacific Ocean, *Nature*, 339, 687-689, 1989.
- [7] Jaffe, D. A., T. Anderson, D. Covert, R. Kotchenruther, B. Trost, J. Danielson, W. Simpson, T. Berntsen, S. Karlsdottir, D. Blake, J. Harris, G. Carmichael, and I. Uno, Transport of Asian air pollution to North America, *Geophys. Res. Lett.*, 26, 711-714, 1999.
- [8] Talbot, R. W., J. E. Dibb, B. L. Lefer, J. D. Bradshaw, S. T. Sandholm, D. R. Blake, N. J. Blake, G. W. Sachse, J. E. Collins, B. G. Heikes, J. T. Merrill, G. L. Gregory, B. E. Anderson, H. B. Singh, D. C. Thornton, A. R. Bandy, and R. F. Pueschel, Chemical characteristics of continental outflow from Asia to the troposphere over the western Pacific Ocean during February-March 1994: Results from PEM-West B. *J. Geophys. Res.* 102, 28255-28274, 1997.
- [9] Kidwell, K.B., NOAA Polar Orbiter Data Users Guide, US Dept. of Commerce, NOAA, 1998.
- [10] Hsu, N.C., J.R. Herman, O. Torres, B.N. Holben, D. Tanre, T.F. Eck, A. Smirnov, B. Chatenet, F. Lavenu, Comparison of the TOMS aerosol index with Sun-photometer aerosol optical thickness: Results and applications," *J. Geophys. Res.*, 105, 6269-6279, 1999.
- [11] Hsu, N.C., J.R. Herman, J.F. Gleason, O. Torres, and C.J. Sefator, Satellite detection of smoke aerosols over a snow/ice surface by TOMS, *Geophys. Res. Lett.* 26, 1165, 1999.